Journal of Electroanalytical Chemistry 634 (2009) 82–89

Contents lists available at ScienceDirect

Journal of Electroanalytical Chemistry

journal homepage: www.elsevier.com/locate/jelechem

Voltammetry for surface-active ions at polarisable liquid|liquid interfaces

Manuel A. Méndez, Bin Su, Hubert H. Girault *

Laboratoire d'Electrochimie Physique et Analytique, Ecole Polytechnique Fédérale de Lausanne (EPFL), Station 6, CH-1015 Lausanne, Switzerland

ARTICLE INFO

Article history:
Received 20 April 2009
Received in revised form 13 July 2009
Accepted 16 July 2009
Available online 26 July 2009

Keywords:
Adsorption
ITIES
Capacitive current
Gouy–Chapman model
Voltammetry

ABSTRACT

Adsorption of charged species at the interface between two immiscible electrolyte solutions (ITIES) is simulated taking into account both the mutual influence between the potential dependent surface excess charge and the potential distribution between the two phases and the partition equilibrium of the surface-active molecules. The electrical potential profiles are calculated assuming a single adsorption plane separating two electrical diffuse layers following the modified Verwey–Niessen model (MVN). The interfacial boundary potential is obtained from the electroneutrality condition. The interplay between adsorption and partition under steady-state conditions is addressed yielding voltammetric responses for the adsorption–desorption processes along with the faradaic response.

1. Introduction

The specific adsorption–desorption of ions and ion-pairs at the ITIES can be determined by measuring interfacial tension measurements under equilibrium conditions [1–7] but also amperometrically under transient conditions, for example by cyclic voltammetry [8–12]. Different adsorption processes can be coupled to ion transfer processes, such as adsorption followed by transfer *e.g.* in the case of amphiphilic surfactant [9,13–16] or transfer followed by adsorption *e.g.* in the case of polyelectrolyte, polypeptide or dendrimer transfer reactions [17–24]. Furthermore, one of the most biologically relevant systems is that of phospholipid monolayers in which adsorption and facilitated ion transfer reactions are closely related [25–28]. In all the cases, the dependence of the adsorption of ionic surfactants on the applied potential was evident. The analysis of charged species adsorption at ITIES is not an easy task and only few rigorous theoretical descriptions of this phenomenon have been reported [29–31]. Continuing with these efforts, we shall model here the voltammetric response obtained with surface-active ions for which the transfer across the interface is preceded by an adsorption step. Indeed, when the surface-active components are ionic, both adsorption and ion transfer energies are strongly affected by the potential, and in turn strongly affect the phase-boundary potential distribution.

Recently, the effect of the adsorption of charged species on the charge distribution at the ITIES using the classical description of the Gouy–Chapman model (G–C) has been reported [30]. In that model, the relative surface coverage was assumed to be potential-dependent assuming a classical Boltzmann statistics [1,25,32]. Here, this approach is used to estimate the coupling between adsorption and potential distribution in the more general case where the species is allowed to partition from one phase to the next as a function of potential, and to predict the capacitive currents arising from adsorption/desorption processes [29].

2. Theory

2.1. System description

The adsorption of charged species at a planar ITIES located at $x = 0$ is analyzed. We shall consider cationic surfactant molecules (s) assumed to be initially only present in the organic phase ($x > 0$) at a concentration ${}^{b}c_{s}^{o}$. As an additional constraint, the charged moiety of the adsorbed amphiphilic cation is assumed to be located in the aqueous side ($x < 0$) of the interface due to its hydrophilicity. In consequence, adsorption and desorption processes imply the flow of charge across the interface, that ultimately leads to the occurrence of significant adsorptive and/or desorptive currents, as it will be evidenced further in the text.

Fig. 1 illustrates schematically the system under consideration in which an example of the concentration profile (Fig. 1a) is presented when s is partitioned between the two phases. At the same time, the potential profile is shown (Fig. 1b), where clear distinction has to be made between $x = 0$ for distances within the diffuse layer few nanometers thick and $X^{o} = 0$ or $X^{w} = 0$ for distances within the diffusion layer few micrometers thick. The former ($x = 0$) corresponds to the boundary between the two phases whereas

* Corresponding author. Fax: +41 21 693 36 67.
E-mail address: hubert.girault@epfl.ch (H.H. Girault).

0022-0728/$ - see front matter © 2009 Elsevier B.V. All rights reserved.
doi:10.1016/j.jelechem.2009.07.013

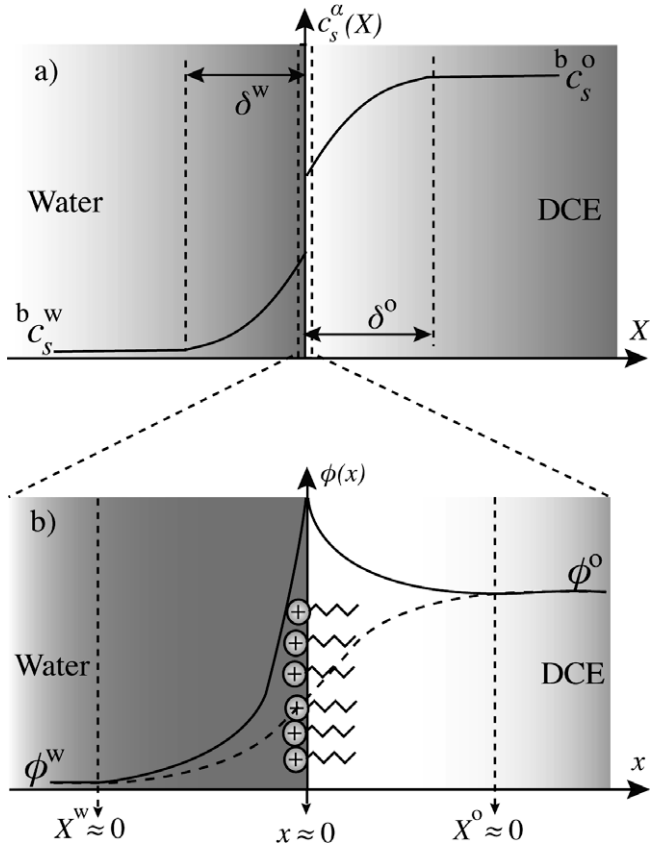

Fig. 1. Schematic representation of (a) the concentration profile and (b) the potential profile across the interface.

$X^{o}\approx 0$ corresponds to the end of the organic electrical diffuse layer referred to $x = 0$. Analogously, $X^{w}\approx 0$ stands for the end of the aqueous electrical double layer. This distinction has to be made since the Nernst equation describing the ratio between the organic and aqueous concentrations of the ions does not take into account the effects of the double electrical layer. When the partition of the charged surfactant is taken into account, close to the interface, the surfactant concentrations on either side of the interface $c^{w}_{s(X^{w}=0)}$ and $c^{o}_{s(X^{o}=0)}$ vary whilst obeying the equality of the fluxes.

2.2. Evaluation of the potential profiles

According to the Verwey–Niessen model, the ITIES can be regarded as two back-to-back diffuse electrical layers, classically described by the G–C theory [33]. As a first approximation, the potential drop across an eventual inner layer separating the two space charge regions is neglected since ions are assumed to be punctual charges. Therefore, the phase-boundary potential corresponds to the potential at $x = 0$ ($\phi_{x=0}$). In all the cases, the initial potential difference water *vs* oil will be taken as positive, *i.e.*, the voltammetric scans will always start from the positive side of the potential window. By convention, the transfer of a positive (negative) charge from the organic (aqueous) phase to the aqueous (organic) phase will produce a net negative (positive) current.

Following the classical G–C theory, in the case of a 1:1 binary supporting electrolyte, the Poisson–Boltzmann equation reads:

$$\frac{\partial^2\phi(x)}{\partial x^2} = \frac{2Fc^{\alpha}}{\varepsilon_0\varepsilon^{\alpha}}\sinh\left\{\frac{F(\phi(x)-\phi^{\alpha})}{RT}\right\} \tag{1}$$

and, after integration, the electric fields in the two diffuse layers of the aqueous and organic phase respectively, of relative permittivities ε^{w} and ε^{o}, correspond to:

$$\left.\frac{\partial\phi(x)}{\partial x}\right|_{-\infty<x\leqslant 0} = \sqrt{\frac{8RTc^{w}}{\varepsilon_0\varepsilon^{w}}}\sinh[f(\phi(x)-\phi^{w})] \tag{2}$$

$$\left.\frac{\partial\phi(x)}{\partial x}\right|_{0<x<\infty} = -\sqrt{\frac{8RTc^{o}}{\varepsilon_0\varepsilon^{o}}}\sinh[f(\phi(x)-\phi^{o})] \tag{3}$$

In Eqs. (2) and (3) ε_0 is the vacuum permittivity, R the gas constant, T the absolute temperature. c^{w} and c^{o} represent the bulk concentrations of the supporting electrolyte in the aqueous and organic phases, respectively. The term f stands for $F/2RT$ where F is the Faraday constant.

At the same time, the electroneutrality condition must always be fulfilled and reads:

$$\sigma^{w} + \sigma^{o} = 0 \tag{4}$$

where the surface charge densities of the aqueous (σ^{w}) and organic (σ^{o}) diffuse layers are derived from the Gauss theorem:

$$\begin{aligned}\sigma^{w} &= -\varepsilon_0\varepsilon^{w}\left.\frac{\partial\phi(x)}{\partial x}\right|_{x=0} + \sigma^{ads}\\ &= -\sqrt{8RT\varepsilon_0\varepsilon^{w}c^{w}}\sinh[f(\phi_{x=0}-\phi^{w})] + \sigma^{ads}\end{aligned} \tag{5}$$

$$\sigma^{o} = -\varepsilon_0\varepsilon^{o}\left.\frac{\partial\phi(x)}{\partial x}\right|_{x=0} = -\sqrt{8RT\varepsilon_0\varepsilon^{o}c^{o}}\sinh[f(\phi_{x=0}-\phi^{o})] \tag{6}$$

$$\sigma^{ads} = z_sF\Gamma_{max}\theta \tag{7}$$

The surface charge density due to the adsorption process (σ^{ads}) is also introduced in the charge balance and explicitly described by Eq. (7), where Γ_{max} represents the maximum surface concentration, θ the relative surface coverage and z_s the charge of the amphiphilic surfactant s. Hence, assuming a Langmuir isotherm, we have:

$$\theta = \frac{\beta c^{o}_{s(X^{o}=0)}}{1+\beta c^{o}_{s(X^{o}=0)}} \tag{8}$$

where β stands for the adsorption coefficient. After substituting Eqs. (7) and (8) into Eq. (5) and further replacement of the expression obtained along with Eq. (6) into the electroneutrality balance, Eq. (4), an expression only dependent on β and $\phi_{(x=0)}$ is obtained. Therefore, if β is assumed to be potential-independent, direct evaluation of the surface potential $\phi_{(x=0)}$ can be performed for a given total potential drop ($\Delta^{w}_{o}\phi = \phi^{w} - \phi^{o}$). However, as reported before [30], when the adsorption coefficient is assumed to be potential-dependent, this equation alone is not sufficient to determine directly the interface boundary potential.

2.3. Adsorption from the organic phase

When the initial potential difference is such that the partition of the amphiphilic charged surfactant can be neglected $\left(i.e.\ {}^{b}c_s^{w}\approx c^{w}_{s(X=0)}\approx 0\right)$, the adsorption will take place only from the organic phase. Then, considering the adsorption as a potential dependent process, the adsorption coefficient, namely β, can be calculated as follows [34]:

$$\beta = \frac{1}{c^{DCE}}\exp\left(-\frac{\Delta G^{\ominus}_{ads}}{RT}\right)\exp\left(\frac{z_sF}{RT}(\phi^{o}-\phi_{x=0})\right) \tag{9}$$

where c^{DCE} corresponds to the concentration of the solvent, *e.g.* 1,2-DCE, in the organic phase and $\Delta G^{\ominus}_{ads}$ to the standard Gibbs energy of adsorption. Eq. (9) can be introduced into Eq. (8) and $\phi_{(x=0)}$ is found as described above.

2.4. Adsorption and ionic partition

When the ionic partition process takes place, the surface concentrations of the charged species on either side of the interface are given by the Nernst equation:

$$\Delta_o^w\phi = \Delta_o^w\phi_{tr,s}^{\theta'} + \frac{RT}{z_sF}\ln\left(\frac{c^o_{s(X^o=0)}}{c^w_{s(X^o=0)}}\right) \tag{10}$$

where $\Delta_o^w\phi_{tr,s}^{\theta'}$ is the formal standard ion transfer potential. Hence, when an external potential is applied, the mass balance for the surfactant s at the interface is given by:

$$D_s^w\left(\frac{\partial c_s^w}{\partial x}\right)_{(X^w=0)} + D_s^o\left(\frac{\partial c_s^o}{\partial x}\right)_{(X^o=0)} = \frac{\partial\Gamma}{\partial t} \tag{11}$$

If the electrochemical experiments are driven at small interfacial areas where spherical diffusion takes place and/or at slow scan rates, transients effects can be neglected. Accordingly, under steady-state conditions the term on the right of the Eq. (10) vanishes. Thus, Eq. (11) can be ultimately expressed as:

$$D_s^w\left(\frac{{}^bc_s^w - c^w_{s(X^w=0)}}{\delta^w}\right) = D_s^o\left(\frac{c^o_{s(X^o=0)} - {}^bc_s^o}{\delta^o}\right) \tag{12}$$

where the contribution of the adsorption process is neglected, according to the considerations mentioned above, leading to the following relationship between the bulk and interfacial concentrations of the surface-active molecule:

$$\left(\frac{\xi_s^w}{\xi_s^o}\right){}^bc_s^w + {}^bc_s^o = \left(\frac{\xi_s^w}{\xi_s^o}\right)c^w_{s(X^w=0)} + c^o_{s(X^o=0)} \tag{13}$$

where the terms ξ_s^w and ξ_s^o stand for the mass transfer coefficients of the surfactant in the aqueous (D_s^w/δ^w) and organic (D_s^o/δ^o) phase, respectively. Considering here the case of a highly lipophilic cation initially present at the organic phase with a scan direction going from positive to negative potentials, *i.e.* ${}^bc_s^w = 0$, Eq. (13) can be simplified and combined with Eq. (10) to yield:

$$c^o_{s(X^o=0)} = \frac{{}^bc_s^o}{1 + r\exp\left[\frac{z_sF}{RT}\left(\Delta_o^w\phi_{tr,s}^{\theta'} - \Delta_o^w\phi\right)\right]} \tag{14}$$

being $r = \xi_s^w/\xi_s^o$. Analogously, after substituting Eqs. (9) and (14) into Eq. (8), an isotherm equation similar to that proposed by Higgins and Corn [34] that includes not only the potential dependent adsorption Gibbs energy term but also an additional term linked to the ionic partition is obtained.

$$\theta_{ss} = \frac{{}^bc_s^o}{c^{DCE}} \times \frac{\exp\left[-\frac{\Delta G^{\ominus}_{ads}}{RT}\right]\exp\left[\frac{z_sF}{RT}(\phi^o - \phi_{x=0})\right]}{\left(1 + r\exp\left[\frac{z_sF}{RT}(\Delta_o^w\phi_{tr,s}^{\theta'} - \Delta_o^w\phi)\right]\right)\left(1 + \frac{{}^bc_s^o}{c^{DCE}}\frac{\exp\left[-\frac{\Delta G^{\ominus}_{ads}}{RT}\right]\exp\left[\frac{z_sF}{RT}(\phi^o - \phi_{x=0})\right]}{1 + r\exp\left[\frac{z_sF}{RT}(\Delta_o^w\phi_{tr,s}^{\theta'} - \Delta_o^w\phi)\right]}\right)} \tag{15}$$

where θ_{ss} corresponds to the relative surface coverage under steady-state conditions. It must also be remarked that if the ion transfer reaction as well as the adsorption process are all electrochemically reversible, the Nernst equation and consequently the adsorption isotherm described by Eq. (15), retain their validities for the surface concentrations of s under transient potential conditions. It is also clear that in the cases where $\Delta G^{\ominus}_{ads}$ assumes extreme negative values (very strong adsorption takes place), the relative surface coverage will tend to unity regardless of the applied external potential [29,30].

2.5. Desorptive current and differential capacitance

The differential capacitance (C_d) is obtained as [30,35]:

$$\frac{1}{C_d} = \frac{1}{C_w} + \frac{1}{C_o} \tag{16}$$

where

$$C_w = \frac{d\sigma}{d\Delta^w_{x=0}\phi} = -\frac{d\sigma^w}{d(\phi_{x=0} - \phi^w)} \tag{17}$$

$$C_o = \frac{d\sigma}{d\Delta_o^{x=0}\phi} = \frac{d\sigma^o}{d(\phi_{x=0} - \phi^o)} \tag{18}$$

Thus, from the surface charge densities calculated for the aqueous and organic diffuse layers and presented in Eqs. (5)–(7), it is possible to obtain the total differential capacitance. In the case of linear sweep voltammetry, the capacitive current density stemming from the adsorption process corresponds to [36]:

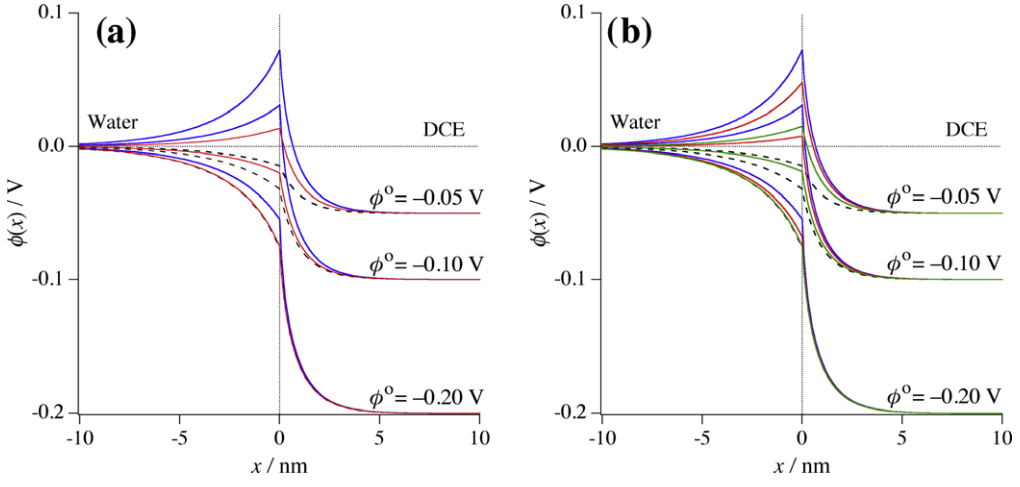

Fig. 2. Potential profiles in the presence of adsorption calculated for (a) $\Delta G^{\ominus}_{ads}$ values of −30 (red) and −40 (blue) kJ mol^{-1} with $c_s^o = 5\times10^{-2}$ mol m^{-3} and for (b) c_s^o values of 2×10^{-3} (green), 1×10^{-2} (red) and 5×10^{-2} (blue) mol m^{-3} with $\Delta G^{\ominus}_{ads} = -40$ kJ mol^{-1}. The profiles in the absence of adsorption are presented as dashed lines in both cases. (For interpretation of the references to colour in this figure legend, the reader is referred to the web version of this article.)

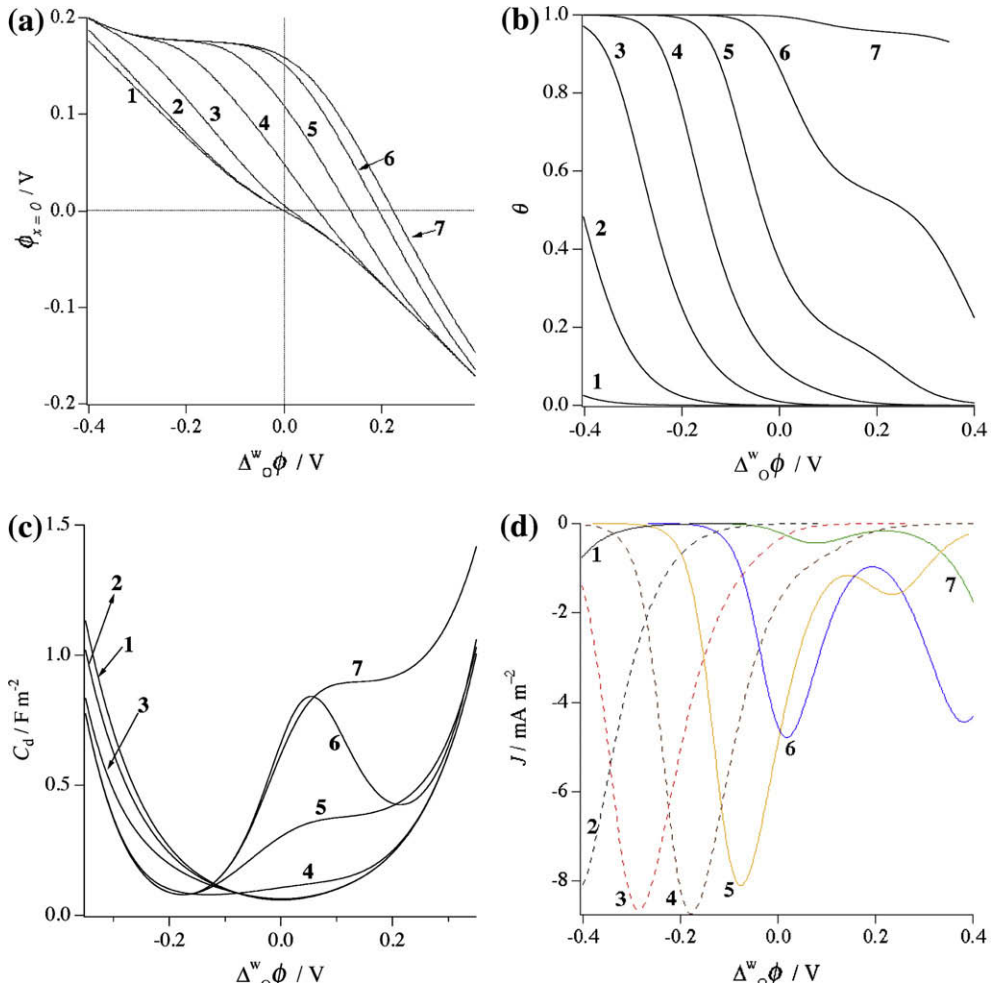

Fig. 3. (a) $\phi_{x=0}$, (b) θ, (c) C_d and (d) steady-state current density (J) as a function of $\Delta^w_o\phi$ at various values of ΔG^e_{ads}; $c^o_s = 5 \times 10^{-2}$ mol m^{-3} and $\Delta G^e_{ads} = 0$ (1), −10 (2), −20 (3), −30 (4), −40 (5), −50 (6) and −60 (7) kJ mol^{-1}.

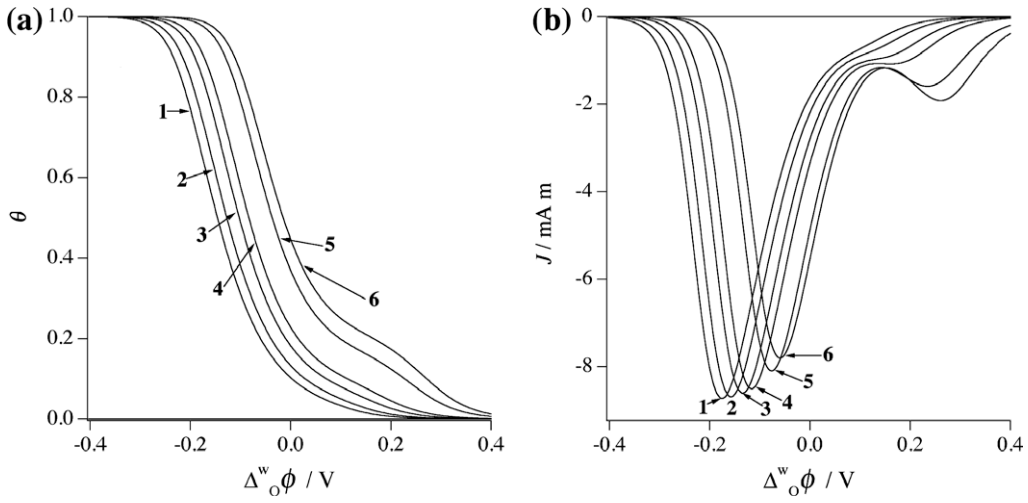

Fig. 4. (a) θ and (b) steady-state current density (J) as a function of $\Delta^w_o\phi$ at various values of c^o_s; $\Delta G^e_{ads} = -40$ kJ mol^{-1} and $c^o_s = 0.1$ (1), 0.2 (2), 0.5 (3), 1 (4), 5 (5) and 10 (6) $\times 10^{-2}$ mol m^{-3}.

$$J_C = \frac{i_C}{A} = \frac{dQ}{dt} = -z_s F \frac{d\Delta^w_o\phi}{dt}\frac{d\Gamma}{d\Delta^w_o\phi} = -z_s F \nu \Gamma_{max}\frac{d\theta}{d\Delta^w_o\phi}$$
$$\approx -z_s F \nu \Gamma_{max}\frac{d\theta_{ss}}{d\Delta^w_o\phi} \quad (19)$$

where A represents the interfacial area, Q the adsorbed charge, ν the sweep rate and Γ the surface concentration. Here, the variation of surface potential with the applied Galvani potential difference is assumed as a first approximation to be equal to the variation of the steady-state value. Also, the steady-state faradaic current will depend on the surface concentration given by:

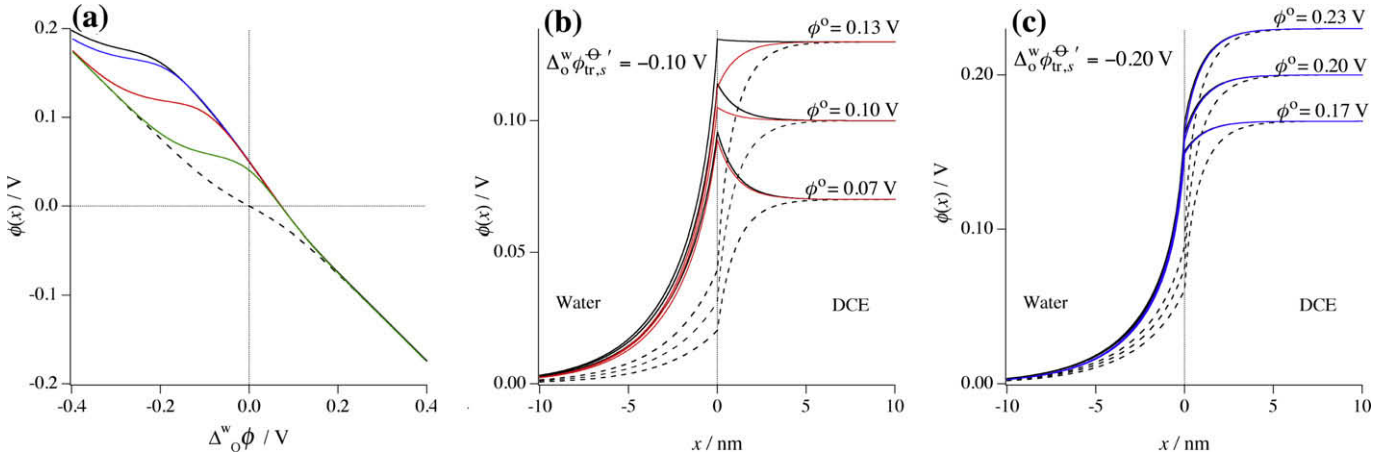

Fig. 5. (a) $\phi_{x=0}$ and (b, c) potential profiles in the presence of adsorption calculated for $\Delta G^o_{ads} = -40$ kJ mol^{-1} and $c^o_s = 1 \times 10^{-3}$ mol m^{-3}. In (a) $\Delta^w_o\phi^{o'}_{tr,s} = -0.20$ (green), -0.10 (blue) and 0 (red) V. In all the cases, the curves obtained in the absence of adsorption are presented as dashed lines. Those calculated in the presence of adsorption but without considering ionic partition are presented as solid black lines. (For interpretation of the references to colour in this figure legend, the reader is referred to the web version of this article.)

$$J_F = \frac{i_F}{A} = z_s F D^o_s \left(\frac{{}^b c^o_s - c^o_{s(X^o=0)}}{\delta^o} \right) \tag{20}$$

which in turn after being combined with Eq. (10) gives:

$$J_F = \frac{i_F}{A} = J_{\lim,F} \frac{1}{1 + \exp\left[\frac{z_s F}{RT}\left(\Delta^w_o\phi - \Delta^w_o\phi^{o'}_{tr,s}\right)\right]} \tag{21}$$

where

$$J_{\lim,F} = -z_s F \varsigma^{ob}_s c^o_s \tag{22}$$

Finally, the total current is calculated as the sum of both contributions, faradaic and capacitive, as follows:

$$J = J_C + J_F \tag{23}$$

3. Theoretical results and discussion

All the results presented herein were obtained using Mathematica 6.0.3 (Wolfram Research Inc.). The values of the parameters used in the calculations presented below are as follows: $T = 298$ K; $z_s = 1$; $\Gamma_{max} = 1.76 \times 10^{-6}$ mol m^{-2}; $v = 0.01$ V s^{-1}; $\varepsilon^o = 10.4$; $\varepsilon^w = 78.54$ and $c^w = c^o = 10$ mol m^{-3}.

The maximum surface coverage value was chosen to be within the range estimated by cyclic voltammetry for the maximum surface coverage of L-α-dipalmitoyl phosphatidylcholine [26], which is well-known for its strong amphiphilic character at the water–DCE interface.

First, no ionic partition was considered. Fig. 2 shows the potential profiles in the absence (dashed lines) and presence of adsorption (solid lines). These were calculated for different values of $\Delta G^{\ominus}_{ads}$ for a fixed value of ${}^b c^o_s$ (a) and *vice versa* (b) at three different total potential drop values. As it can be seen, the potential distribution is clearly inverted at $\phi^o = -0.05$ V, since $\phi_{(x=0)}$ increases with σ^{ads} [3,37]. Therefore, this inversion effect is enhanced for higher values of either $\Delta G^{\ominus}_{ads}$ or c^o_s due to the increase in θ and consequently in σ^{ads}, as observed from Fig. 3a and b [38]. At the same time, the capacity measurements indicate an enhancement of the double layer capacity caused by the increase in the charge density, mainly at positive potentials for highly negative values of $\Delta G^{\ominus}_{ads}$ (Fig. 3c).

Simultaneously, Fig. 3d shows that at very negative values of $\Delta G^{\ominus}_{ads}$, no significant adsorptive or desorptive currents are obtained

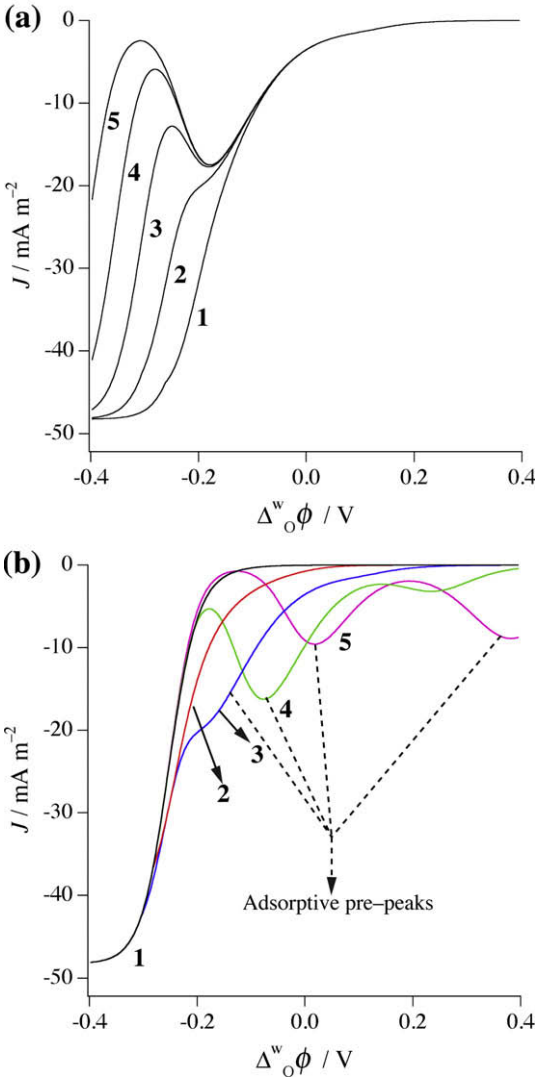

Fig. 6. Steady-state current density (J) as a function of $\Delta^w_o\phi$ calculated for (a) a constant value of $\Delta G^{\ominus}_{ads} = -30$ kJ mol^{-1} and values of $\Delta^w_o\phi^{o'}_{tr,s} = -0.20$ (1), -0.25 (2), -0.30 (3), -0.35 (4) and -0.40 (5) V. In (b) $\Delta^w_o\phi^{o'}_{tr,s} = -0.25$ V and $\Delta G^{\ominus}_{ads} = -10$ (1), -20 (2), -30 (3), -40 (4) and -50 (5) kJ mol^{-1}. In all the cases ${}^b c^o_s = 5 \times 10^{-2}$ mol m^{-3}, $r = 1$ and $v = 20$ mV s^{-1}.

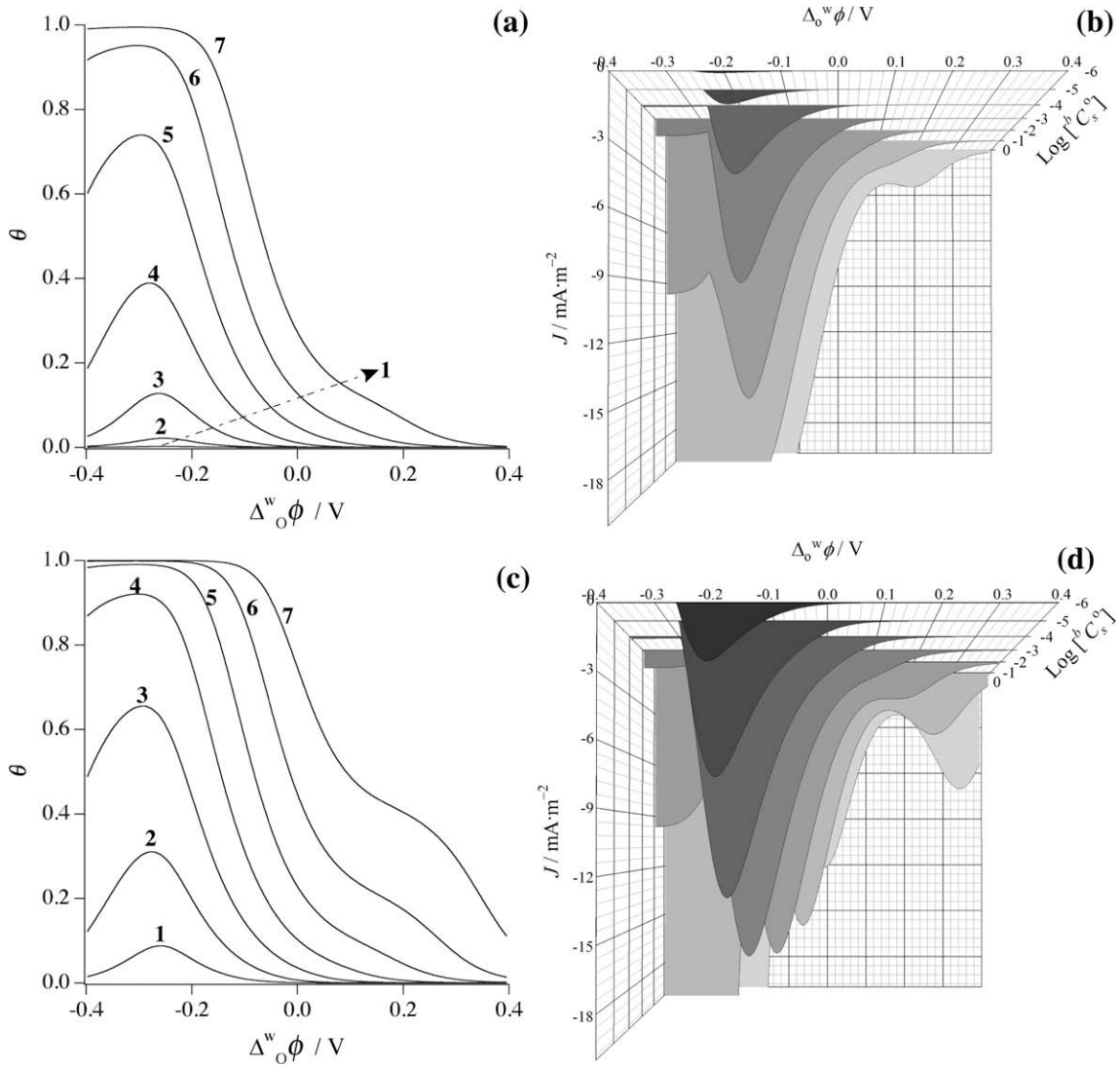

Fig. 7. (a, c) θ and (b, d) steady-state current density (J) as a function of $\Delta_o^w\phi$ at various values of c_s^o; (a, b) $\Delta G_{ads}^{\theta} = -30$ kJ mol^{-1}, (c, d) $\Delta G_{ads}^{\theta} = -40$ kJ mol^{-1}. In (a) and (c) $c_s^o = 0.001$ (1), 0.01 (2), 0.1 (3), 1 (4), 10 (5), 100 (6) and 1000 (7) $\times 10^{-3}$ mol m^{-3}. In all the cases, $\Delta_o^w\phi_{tr,s}^{\theta'} = -0.25$ V , $r = 1$ and $v = 20$ mV s^{-1}.

since the adsorption process becomes nearly potential-independent (Fig. 3b, curve 7), whereas at values of ΔG_{ads}^{θ} close to zero no appreciable desorptive signals are observed due to the low relative surface coverage (Fig. 3b, curve 1). However, at intermediate values of ΔG_{ads}^{θ}, the relative coverage lowers at rather positive potentials, where $\phi^o - \phi_{(x=0)} < 0$, defining a potential-independent adsorption zone. At the same time, a potential dependent adsorption zone appears from approximately $\Delta_o^w\phi < 0$ in all the cases. At slightly positive potentials and rather negative values of ΔG_{ads}^{θ} (*e.g.* Fig. 3b, curve 5) the overlapping of these two zones occurs, inducing the appearance of a shoulder in the relative surface coverage profile. Equivalent results are obtained for a constant value of ΔG_{ads}^{θ} and increasing concentrations of the surfactant, ${}^b c_s^o$ (Fig. 4a).

Furthermore, Fig. 4b shows that an increase in the concentration of the surfactant shifts the desorptive current peak potential towards more positive values of $\Delta_o^w\phi$. The behavior of the transition zone between potential–dependent and independent zones will induce the deformation of the peaks. As a result, asymmetric or even double adsorptive current signals are observed in the simulated linear scan voltammogram (Fig. 4b).

In stark contrast, when the ionic partition of the surfactant is considered, $\phi_{(x=0)}$ tends to match the values obtained in absence of adsorption at potentials more negative than $\Delta_o^w\phi_{tr,s}^{\theta'}$ (Fig. 5a, green and red curves). Consequently, significant differences between the potential profiles calculated with and without considering ionic partition will only be observed at moderately negative $\Delta_o^w\phi_{tr,s}^{\theta'}$ values. For instance, when $\Delta_o^w\phi_{tr,s}^{\theta'} = -0.1$ V (Fig. 5b), the potential profiles calculated 30 mV before ($\Delta_o^w\phi = -0.07$ V $\Longleftrightarrow$ $\phi^o = 0.07$ V) and after ($\Delta_o^w\phi = -0.13$ V $\Longleftrightarrow$ $\phi^o = 0.13$ V) this value reveal major changes mainly at $\Delta_o^w\phi \leqslant \Delta_o^w\phi_{tr,s}^{\theta'}$. The latter can be explained from the depletion of s in the organic phase caused by the ionic partition process in this potential region, which ultimately leads to lower surface coverages and therefore to smaller effects on the potential profiles.

However, as s becomes increasingly hydrophobic, *i.e.* $\Delta_o^w\phi_{tr,s}^{\theta'}$ turns more negative, this trend vanishes. Under these circumstances, the calculated $\phi_{(x=0)}$ values closely resemble those obtained upon neglecting ionic partition rather than those in the absence of adsorption (Fig. 4a, blue curve). As a consequence, no appreciable differences between the potential profiles calculated for the cases in which s is confined in the organic phase or allowed to partition are evidenced; which can be clearly seen in Fig. 4c for a $\Delta_o^w\phi_{tr,s}^{\theta'}$ value of -0.2 V.

Furthermore, the current signal stemming from the surfactant adsorption can only be discerned from the faradaic currents when

the standard ion transfer potential adopts considerable negative values, *i.e.*, when the surfactant as a whole is very hydrophobic (Fig. 6a). In general, the potential at which the adsorptive current signal is registered does not depend on $\Delta_o^w\phi^{o'}_{tr,s}$ whereas it is strongly affected by ΔG^o_{ads}. Accordingly, adsorptive pre-peaks are exhibited in the linear scan voltammograms.

After varying the ΔG^o_{ads} values at a fixed $\Delta_o^w\phi^{o'}_{tr,s}$ (Fig. 6b), the evolution of the current potential curves can be appreciated and two main cases can be distinguished: on the one hand, at slightly negative values of ΔG^o_{ads} ($\geqslant -20$ kJ mol^{-1}), rather than a well-defined adsorptive peak, the voltammograms show the merging of both, capacitive and faradaic currents, into a single wave which shape differs from the ideal case where there is no adsorption. This behavior is indicative of the close potential-proximity between the adsorptive and diffusive events. On the other hand, as ΔG^o_{ads} becomes more negative, a bigger separation between the capacitive and faradaic contributions occurs. As a matter of fact, at extremely negative values, an additional current peak can be observed at the positive edge of the potential window. The latter being caused by the potential-independent adsorption of the surfactant, as discussed before.

Another important parameter to consider is the concentration of the surfactant. After computing the relative surface coverage and current density curves, three remarkable facts are appreciated in these results and summarized in Fig. 7:

- First, the organic bulk concentration of s ($^bc^o_s$) significantly alters the capacitive current, being especially sensitive at low values where the presence of triangular-shaped current peaks is evident. Nevertheless, once $^bc^o_s$ exceeds a certain threshold, the adsorptive current density remains approximately constant whereas the faradaic current will keep increasing linearly with the concentration. In a later stage, at high concentrations, the diffusive current prevails over that stemming from the surfactant adsorption until complete masking of the capacitive currents takes place (Fig. 7b).
- Second, peak-shaped relative surface coverage profiles are obtained. The latter, due to the depletion of the surfactant concentration in the organic phase caused by the transfer and diffusion of the surface-active ion into the aqueous phase, as discussed before. Moreover, the potential of maximum surface coverage attainment turns out to be dependent on $^bc^o_s$. Indeed, at low concentrations the maximum surface coverage is reached at the standard formal ion transfer potential, as predicted by Kakiuchi [29].
- Third, when strong adsorption occurs, *i.e.* at very negative ΔG^o_{ads} values (*e.g.* -40 kJ mol^{-1}), there is a shift towards less negative potentials in the maximum of the capacitive response as the concentration increases (Fig. 7d). This can also be clearly appreciated in the relative surface coverage curve, where it must also be remarked that even when equilibrium conditions are being assumed throughout the calculations, this anodic shift can be presented and must not be confused with a deviation from the electrochemical reversibility of the ion transfer reaction. Nevertheless, experimental discernment between adsorption processes and kinetic limitations might not be trivial, especially when close potential-vicinity between adsorptive and faradaic current signals occurs.

Finally, it is clear that only at low concentrations the capacitive contributions are predominant. In consequence, adsorption-diagnostic signals primordially appears when both, low concentrations and high scan rates are employed within the course of the electrochemical measurements (Fig. 7b and d).

As it can be inferred from Eq. (19), the adsorptive current is proportional to the scan rate while the steady-state faradaic current is scan rate-independent. The overall response obtained at different scan rates, ranging from 2 to 50 mV s^{-1}, is shown in Fig. 8 where the above-described behavior is evidenced.

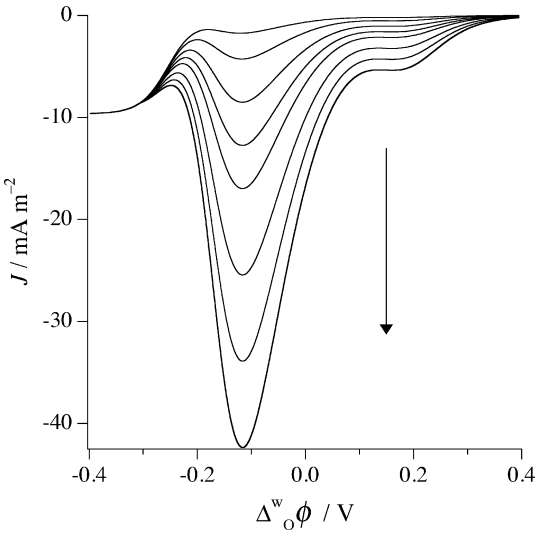

Fig. 8. Steady state current density (J) as a function of $\Delta_o^w\phi$ obtained for $\Delta_o^w\phi^{o'}_{tr,s} = -0.25$ V for different values of v; $r = 1$, $\Delta G^o_{ads} = -30$ kJ mol^{-1}, $^bc^o_s = 5 \times 10^{-2}$ mol m^{-3} and $v = 2$, 5, 10, 15, 20, 30, 40 and 50 mV s^{-1}. The arrow indicates the direction of the scan rate increase.

In summary, when ionic partition is considered under steady-state conditions the adsorption process gives rise to peak-shaped relative surface coverage profiles whose maximum will greatly depend on ΔG^o_{ads} but is independent on $\Delta_o^w\phi^{o'}_{tr,s}$. At the same time, capacitive currents stemming from adsorptive/desorptive processes will significantly contribute to the total registered current in voltammetric experiments mainly at low surface–active molecule concentrations and high scan rates.

4. Conclusions

The present model constitutes a generalized model in which the influence over the capacitive current of adsorption/desorption and ionic partition processes is rationalized. It is shown that capacitive currents in the presence of adsorption are significantly altered by the variation of not only the Gibbs energy of adsorption but also by factors like the scan rate and the surfactant concentration. At relatively small values for the adsorption Gibbs energies, the maximum relative surface coverage is generally observed at the standard ion transfer potential. Nevertheless, when the adsorption Gibbs energy dominates over that of the ion transfer process, the adsorption becomes maximum at potentials different from the standard ion transfer potential shifting the adsorptive capacitive current peak towards less negative potentials. Indeed, only in this case the appearance of the desorptive current pre-peaks in voltammetric measurements can be expected. Finally, the present approach also indicates that, depending on the side of the interface at which the charged moiety of the surfactant molecule be located upon adsorption, either pre or post-peaks can be obtained. The latter is in close resemblance to the behavior observed at the solid–liquid interface [39].

Acknowledgements

The Fonds National Suisse pour la Recherche Scientifique is thanked for the financial support through the project "Electrochemical methodology for the study of peptide–lipid interaction" (Grant No. 200020-113428). Professor Takashi Kakiuchi and Pro-

fessor Masahiro Yamamoto are gratefully acknowledged for stimulating discussions; Hubert H. Girault is grateful to Kyoto University for a visiting fellowship.

References

[1] A.G. Volkov, D.W. Deamer, D.L. Tanelian, V.S. Markin, Prog. Surf. Sci. 53 (1996) 1–134.
[2] V.S. Markin, A.G. Volkov, M.I. Volkova-Gugeshashvili, J. Phys. Chem. B 109 (2005) 16444–16454.
[3] A. Trojánek, P. Krtil, Z. Samec, J. Electroanal. Chem. 517 (2001) 77–84.
[4] H.H. Girault, D. Schiffrin, J. Electroanal. Chem. 179 (1984) 277–284.
[5] T. Kakiuchi, M. Nakanishi, M. Senda, Bull. Chem. Soc. Jpn. 61 (1988) 1845–1851.
[6] T. Kakiuchi, M. Nakanishi, M. Senda, Bull. Chem. Soc. Jpn. 62 (1989) 403–409.
[7] Z. Samec, A. Trojánek, P. Krtil, Faraday Discuss. 129 (2005) 301–313.
[8] S. Ulmeanu, H.J. Lee, H.H. Girault, Electrochem. Commun. 3 (2001) 539–543.
[9] T. Kakiuchi, Electrochem. Commun. 2 (2000) 317–321.
[10] H. Nagatani, D.J. Fermın, P.F. Brevet, H.H. Girault, J. Phys. Chem. B 105 (2001) 9463–9473.
[11] M.D. Osborne, H.H. Girault, J. Electroanal. Chem. 370 (1994) 287–293.
[12] A.I. Azcurra, L.M. Yudi, A.M. Baruzzi, J. Electroanal. Chem. 461 (1999) 194–200.
[13] T. Goto, K. Maeda, Y. Yoshida, Langmuir 21 (2005) 11788–11794.
[14] M. Shinshi, T. Sugihara, T. Osakai, M. Goto, Langmuir 22 (2006) 5937–5944.
[15] M.Y. Vagin, S.A. Trashin, S.Z. Ozkan, G.P. Karpachova, A.A. Karyakin, J. Electroanal. Chem. 584 (2005) 110–116.
[16] G. Herzog, V. Kam, D.W.M. Arrigan, Electrochim. Acta 53 (2008) 7204–7209.
[17] A. Berduque, M.D. Scanlon, C.J. Collins, D.W.M. Arrigan, Langmuir 23 (2007) 7356–7364.
[18] H. Nagatani, T. Ueno, T. Sagara, Electrochim. Acta 53 (2008) 6428–6433.
[19] T. Osakai, H. Yamada, H. Nagatani, T. Sagara, J. Phys. Chem. C 111 (2007) 9480–9487.
[20] S. Amemiya, X. Yang, T.L. Wazenegger, J. Am. Chem. Soc. 125 (2003) 11832–11833.
[21] Y. Yuan, S. Amemiya, Anal. Chem. 76 (2004) 6877–6886.
[22] R.A. Iglesias, S.A. Dassie, A.M. Baruzzi, J. Electroanal. Chem. 483 (2000) 157–162.
[23] A.I. Azcurra, L.M. Yudi, A.M. Baruzzi, T. Kakiuchi, J. Electroanal. Chem. 506 (2001) 138–142.
[24] M. Calderon, L.M.A. Monzón, M. Martinelli, A.V. Juarez, M.C. Strumia, L.M. Yudi, Langmuir 24 (2008) 6343–6350.
[25] Y. Yoshida, K. Maeda, O. Shirai, J. Electroanal. Chem. 578 (2005) 17–24.
[26] H. Jänchenová, K. Stulik, V. Marecek, J. Electroanal. Chem. 612 (2008) 186–190.
[27] M.A. Méndez, M. Prudent, B. Su, H.H. Girault, Anal. Chem. 80 (2008) 9499–9507.
[28] R.J. Roozeman, L. Murtomäki, K. Kontturi, J. Electroanal. Chem. 575 (2005) 9–17.
[29] T. Kakiuchi, J. Electroanal. Chem. 496 (2001) 137–142.
[30] B. Su, N. Eugster, H.H. Girault, J. Electroanal. Chem. 577 (2005) 187–196.
[31] A. Mälkiä, P. Liljeroth, A.K. Kontturi, K. Kontturi, J. Phys. Chem. B 105 (2001) 10884–10892.
[32] Z. Samec, A. Trojánek, H.H. Girault, Electrochem. Commun. 5 (2003) 98–103.
[33] Z. Samec, Chem. Rev. 88 (1988) 617–632.
[34] D.A. Higgins, R.M. Corn, J. Phys. Chem. B 97 (1993) 489–493.
[35] H.A. Santos, V. Garcia-Morales, L. Murtomäki, J. Electroanal. Chem. 599 (2007) 194–202.
[36] V. Marecek, A. Lhotsky, H. Janchenova, J. Phys. Chem. B 107 (2003) 4573–4578.
[37] H.A. Santos, S. Carlsson, L. Murtomäki, K. Kontturi, ChemPhysChem 8 (2007) 913–920.
[38] T. Kakiuchi, M. Kobayashi, M. Senda, Bull. Chem. Soc. Jpn. 60 (1987) 3109–3114.
[39] R.H. Wopschall, I. Shain, Anal. Chem. 39 (1967) 1514–1527.